# Supporting Information

## Enhanced Cell Capture on Functionalized Graphene Oxide Nanosheets through Oxygen Clustering

Neelkanth M. Bardhan[†,‡,¶,§], Priyank V. Kumar[†,§,⊿], Zeyang Li[‖], Hidde L. Ploegh[‖,⊥], Jeffrey C. Grossman[*,†], Angela M. Belcher[*,†,‡,¶] and Guan-Yu Chen[*,#,@]

† Department of Materials Science and Engineering, Massachusetts Institute of Technology, Cambridge, MA 02139, USA

‡ Department of Biological Engineering, Massachusetts Institute of Technology, Cambridge, MA 02139, USA

¶ The David H. Koch Institute for Integrative Cancer Research at the Massachusetts Institute of Technology, Cambridge, MA 02139, USA

‖ Whitehead Institute for Biomedical Research, Cambridge, MA 02142, USA

⊥ Department of Biology, Massachusetts Institute of Technology, Cambridge, MA 02139, USA

# Institute of Biomedical Engineering, National Chiao Tung University, Hsinchu, Taiwan 30010

@ Department of Biological Science and Technology, National Chiao Tung University, Hsinchu, Taiwan 30010

⊿ Current address: Optical Materials Engineering Laboratory, ETH Zurich, 8092 Zurich, Switzerland

* Corresponding Authors: belcher@mit.edu, jcg@mit.edu, guanyu@nctu.edu.tw

§ These authors contributed equally to this work.

# Contents

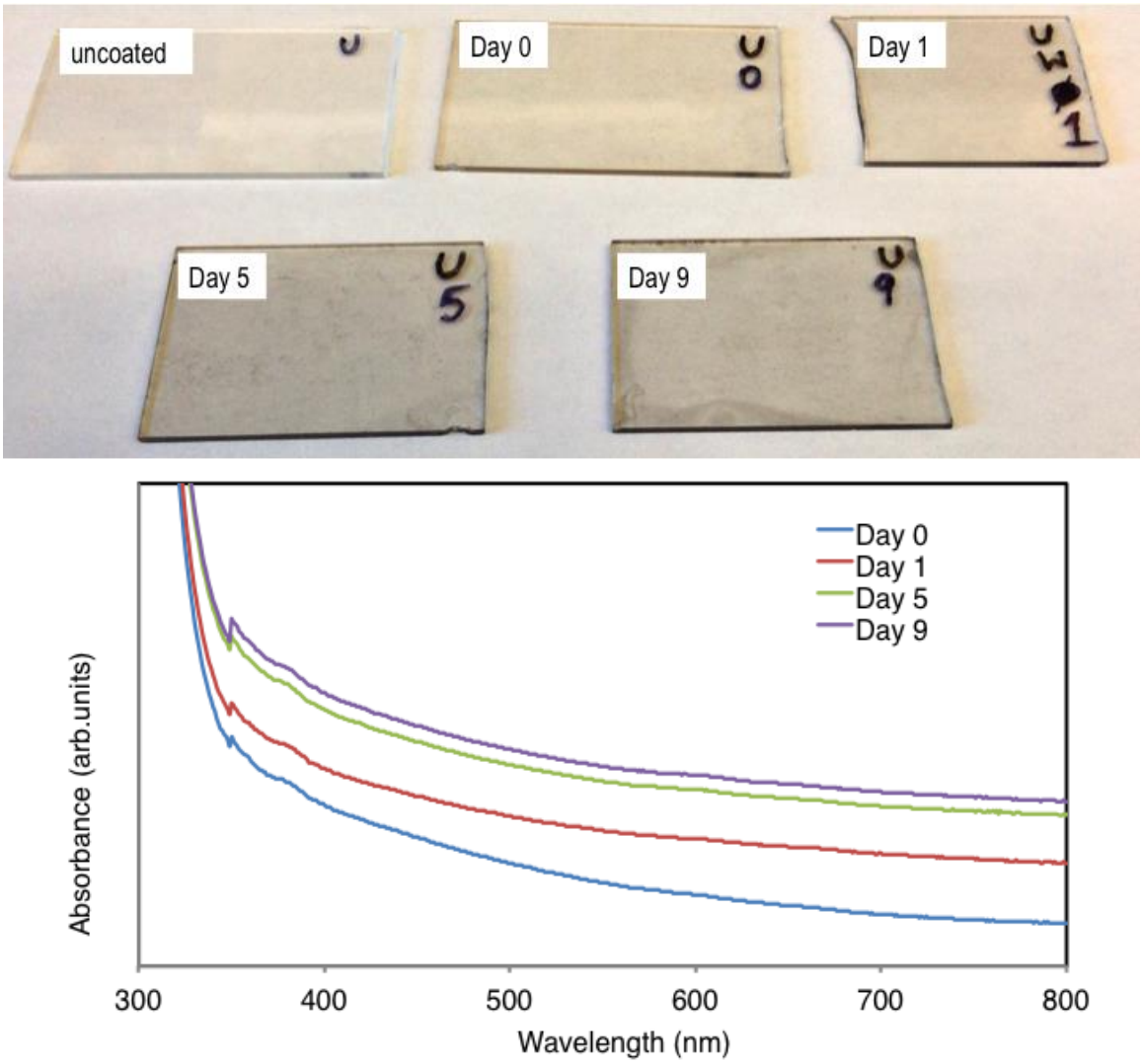


**Figure S1. Effect of thermal annealing on the optical properties of coated glass substrates.** Digital photographs of GO-coated glass slides at different stages of mild annealing at 80 °C. The slides become darker gradually with annealing time (from day 0 to day 9). The UV-vis absorbance measurements confirm an increase in visible absorption with annealing time, consistent with the darkening of the samples. An uncoated glass slide is shown for reference. The black markings/characters on the glass slides were used for internal referencing purposes and should kindly be disregarded.

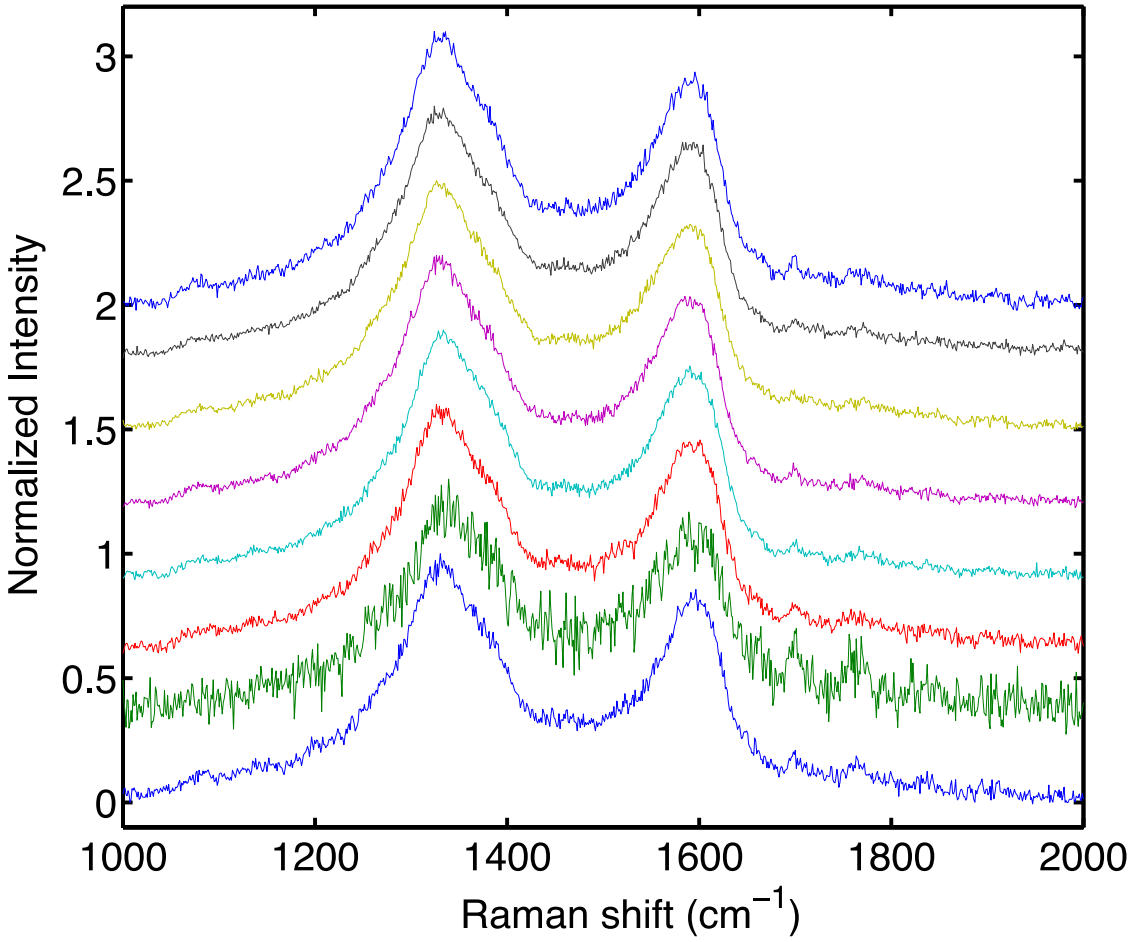


**Figure S2. Raman spectra demonstrating uniformity of GO-coated substrates.**
Raman spectra acquired at eight different randomly chosen points on a GO-coated glass slides. The presence of the *D*- (~ 1350 cm$^{-1}$) and *G*-bands (~ 1600 cm$^{-1}$) in the spectra is a signature of GO structures and indicates that the assembly of GO nanosheets is continuous and that the pin holes are largely absent.

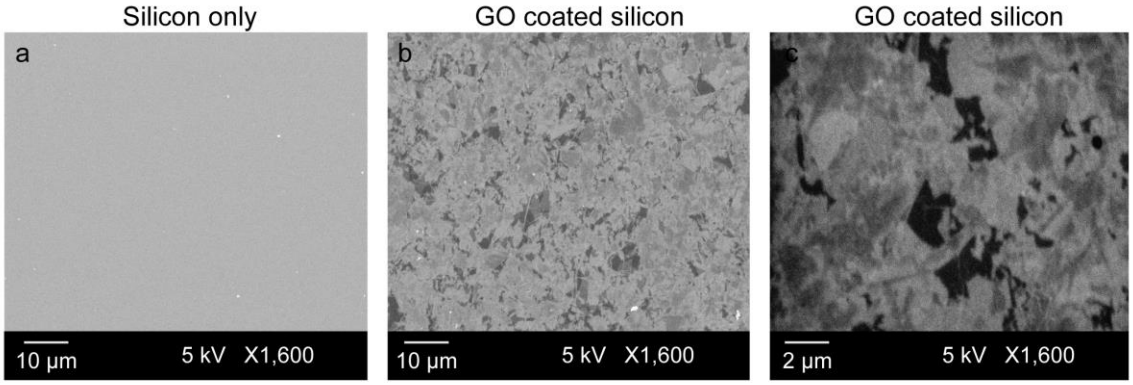


**Figure S3. Scanning electron micrographs of GO immobilized on the substrate.**
**(a)** Silicon wafer ($SiO_2$ layer), **(b, c)** GO on the silicon substrate. Dense coverage of GO on the substrate is revealed in **(b)**. The thin sheet morphology of GO is clearly observed in **(c)**. Scanning electron microscopy (SEM) images of GO nanosheets immobilized on a silicon substrate showed even and dense coverage of thin sheets on the surface, with spacing between adjacent sheets < 2 $\mu$m.

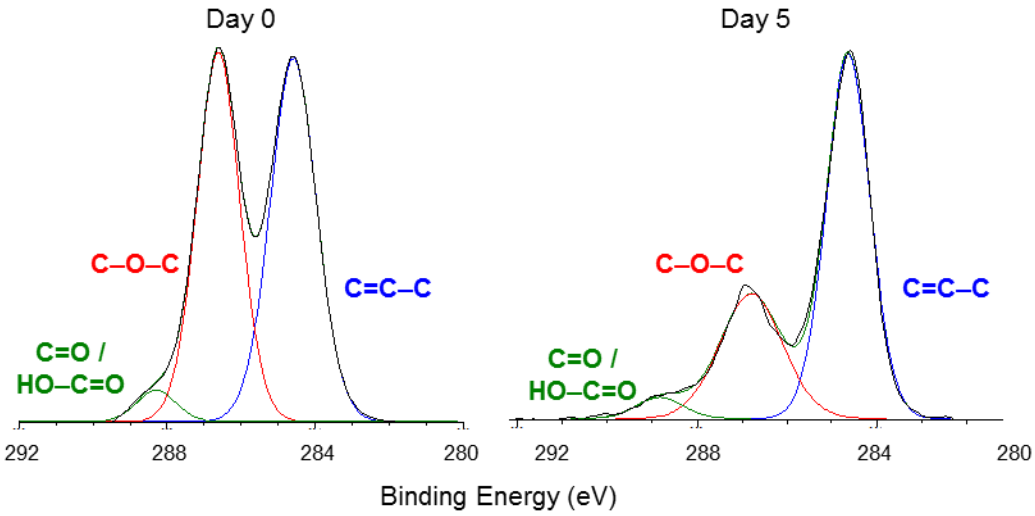


**Figure S4. C 1*s* XPS spectra of *control*- (day 0) and *treated*-GO (day 5) substrates.** The raw spectra were fitted to 3 peaks at 284.6 eV, 286.8 eV and 288.2 eV, respectively attributed to the C=C–C, C–O–C and C=O / HO–C=O bonding chemistries.

**Table S1: Relative fractions of carbon and oxygen elements in the GO.**

| | C (at. %) | O (at. %) |
|---|---|---|
| *Control*-GO (day 0) | 65.8% | 34.2% |
| *Treated*-GO (day 5) | 68.3% | 31.7% |

We note that the calculated oxygen content is ~ 34 at.% and ~ 32 at.%, respectively for the *control*-GO (day 0), and the *treated*-GO (day 5) substrates. The slight decrease in the oxygen content upon thermal annealing has been well documented in the literature. Previously, Kim, S. *et al*.[1] have shown that as-synthesized GO structures are metastable, and undergo a small amount of reduction with time, due to the interaction between oxygen and chemi-sorbed H atoms at room temperature. Subsequently, our own work[2] and reports by other groups[3] have shown that the process of thermal annealing results in a phase separation of the mixed $sp^2$-$sp^3$ phase into distinct oxidized and graphitic domains (which is kinetically accelerated at the temperatures used, ~ 70 - 80 °C by various groups, including the present work), without significant loss in oxygen content[4] which is observed in either thermal or chemical reduction of GO to rGO.

**Table S2: Relative fractions of the various forms of carbon bonds in the GO.**

| | **C=C–C** | **C–O–C** | **C=O / HO–C=O** |
|---|---|---|---|
| Day 0 (*control*-GO) | 45.5% | 50.8% | 3.7% |
| Day 5 (*treated*-GO) | 53.1% | 42.7% | 4.2% |

The relative fractions of the different carbon bonds are shown in Table S2. It is evident that the fraction of epoxide bonding decreases with thermal annealing. The ratio of $sp^2$-bonded carbon increases, as well as the amount of carbon forming carbonyl functional groups, at the expense of the epoxies. This provides further evidence of the phase-separation mechanism (the formation of graphitic regions in *treated*-GO, indicated by the prominent increase in the C=C–C intensity), as well as the enhanced reactivity towards amine functionalization (by the nucleophilic attack mechanism, indicated by the increase in the C=O content). See also Fig. 5(c) in the Main text.

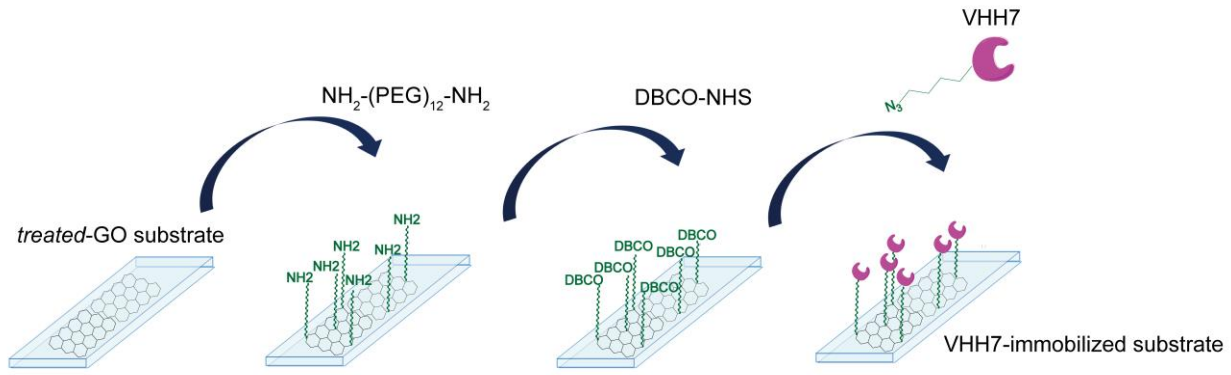


**Figure S5. Schematic of the functionalization procedure of GO.**
The *treated*-GO is activated with N-hydroxysuccinimide (NHS) in a reaction catalyzed by 1-Ethyl-3-(3-dimethylaminopropyl)carbodiimide hydrochloride (EDC). A diamino-polyethylene glycol ($PEG_{12}$) linker is introduced with one end reacting with the N-hydroxysuccinimide (NHS) moiety. The other end of the PEG linker is further functionalized with an NHS-activated dibenzocyclooctyne (DBCO). The VHH7, which has been labeled with an azide in a sortase-catalyzed reaction, is then "clicked" onto the DBCO in a strain-promoted cycloaddition.

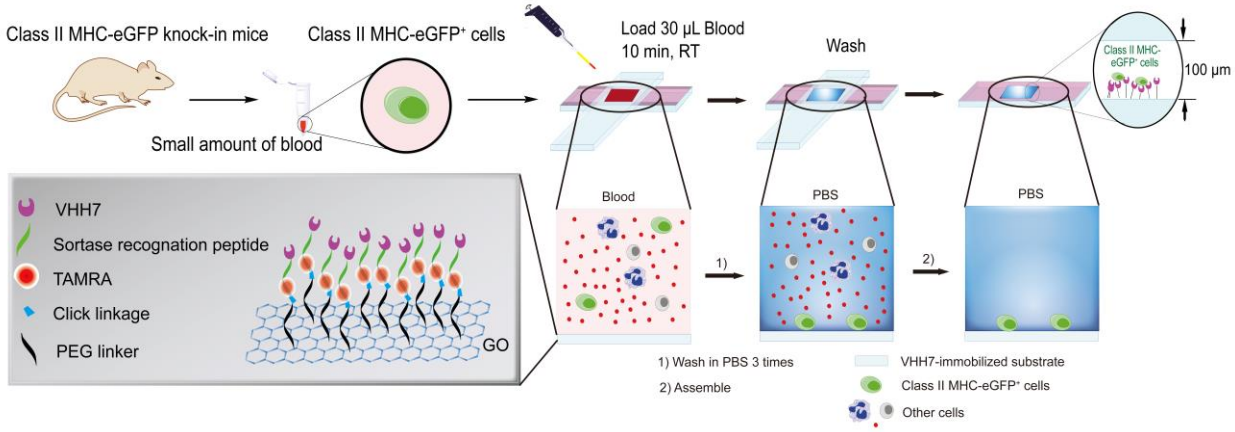


**Figure S6. Mechanism of the capture of cells from whole blood using the VHH7-functionalized GO substrates.**
We used a combination of a sortase-mediated transpeptidation reaction in combination with 'click' chemistry to site-specifically attach a fluorescently labeled VHH via a carboxyterminal LPXTG motif to PEG linker-modified *treated*-GO. We thus installed an anti-murine Class II MHC VHH (VHH7), which sortase-labeled with a TAMRA fluorophore, to *treated*-GO nanosheets. The functionalized surfaces allowed us to selectively capture Class II MHC-eGFP-positive (MHC-$GFP^+$) cells from small volumes (30 $\mu$L) of peripheral blood with minimal handling in a device of simple geometry.

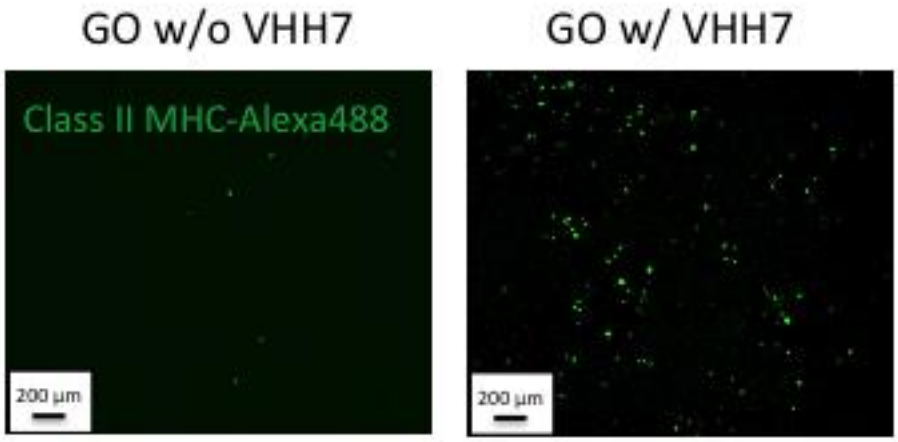


**Figure S7. Role of nanobodies in cell capture from spiked PBS solution.**
Two GO-based cell capture substrates, **(*left*)** without and **(*right*)** with VHH7 antibodies were prepared to verify the important role played by the antibodies in acting as effective binding centers for the cells. A20 (murine Class II $MHC^+$) cells were spiked in PBS and introduced into the cell capture chamber (see main text for Methods). After the cell capture, they were stained with an Alexa 488-labeled anti-Class II MHC antibody for imaging. Each green dot represents a dye-labeled cell. We observe negligible cell capture in the case of the substrates without VHH7, thus confirming VHH7 antibody grafting is necessary to capture murine Class II $MHC^+$ cells. These experiments were performed on as-synthesized (day 0) GO samples. Scale bar is 200 $\mu$m for both images.

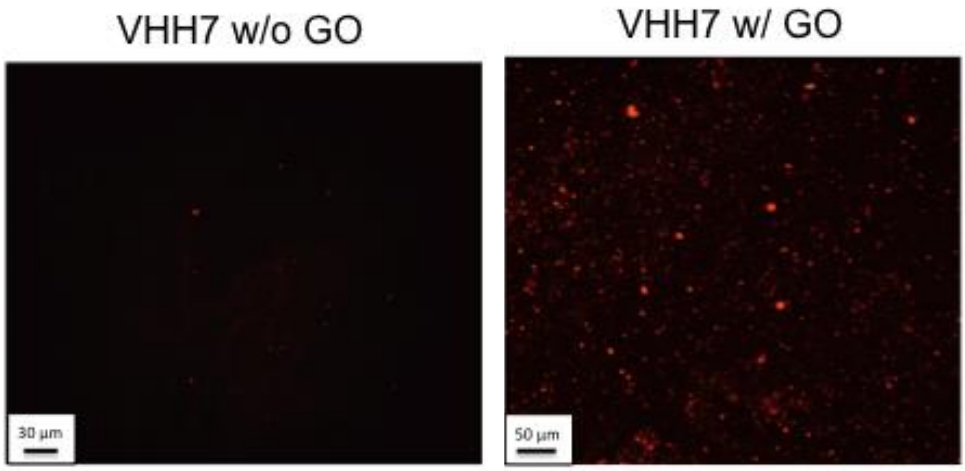


**Figure S8. Role of GO in cell capture.**
Confocal microscopy images of control experiments **(*left*)** without and **(*right*)** with GO nanosheets. VHH7 modified with both a TAMRA moiety and an azide was grafted onto the GO coated or uncoated substrate. The TAMRA signal (left image) and its absence in the right image indicate that GO nanosheets are essential for grafting antibodies onto the substrate and for subsequent cell capture experiments. Scale bar is 30 $\mu$m for left image, and 50 $\mu$m for right image.

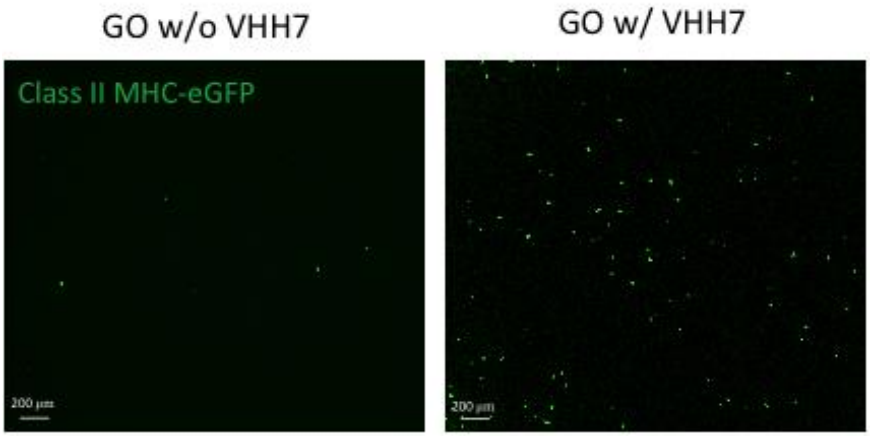


**Figure S9. Role of nanobodies in cell capture from murine whole blood.**
Cell capture on as-synthesized (day 0) GO substrates using Class II MHC-eGFP$^{+}$ whole blood samples, performed at room temperature. In this case, the GFP (green fluorescent protein) markers that are expressed by the captured cells are used to identify them under a confocal microscope. Clearly, ***(left)*** samples without VHH7 indicate negligible cell capture due to the absence of antibodies, compared to ***(right)*** with VHH7 antibodies. Scale bar is 200 $\mu$m for both images.

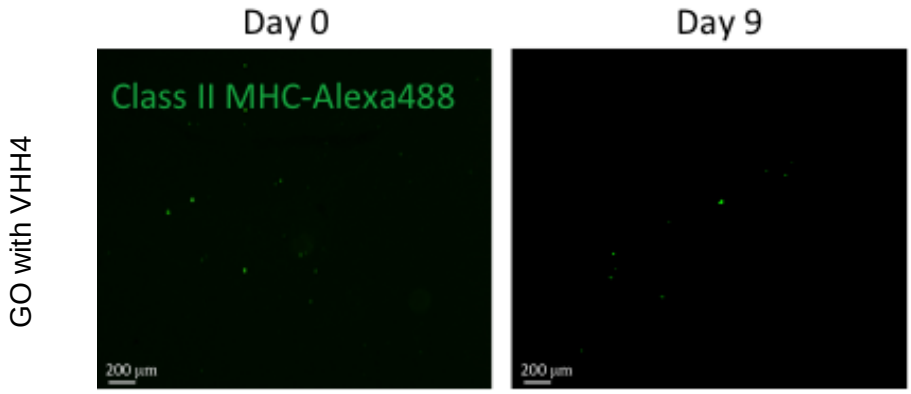


**Figure S10. Enhanced cell capture efficiency correlated to specificity of binding.**
We performed cell capture experiments (using the A20 cell line) on VHH4 grafted GO substrates. VHH4 nanobodies are specific to human Class II MHC$^{+}$ cells and do not bind to murine Class II MHC$^{+}$ cells. We note that this is indeed the case for both day 0 and day 9 samples. As shown above, we do not detect any significant cell binding onto these substrates and furthermore, there is no difference between day 0 and 9 cases. This data further confirms that phase transformation doesn't lead to any non-specific binding and helps us understand that the increase in yield going from day 0 to day 9 on VHH7-immobilized substrate was indeed due to VHH7 on the substrate, and not due to any other phenomenon induced because of phase transformation. For instance, if the increase in capture yield was due to some other phenomenon, we should have observed an increase in yield going from day 0 to day 9, even by switching our system to VHH4. Scale bar is 200 $\mu$m for both images.

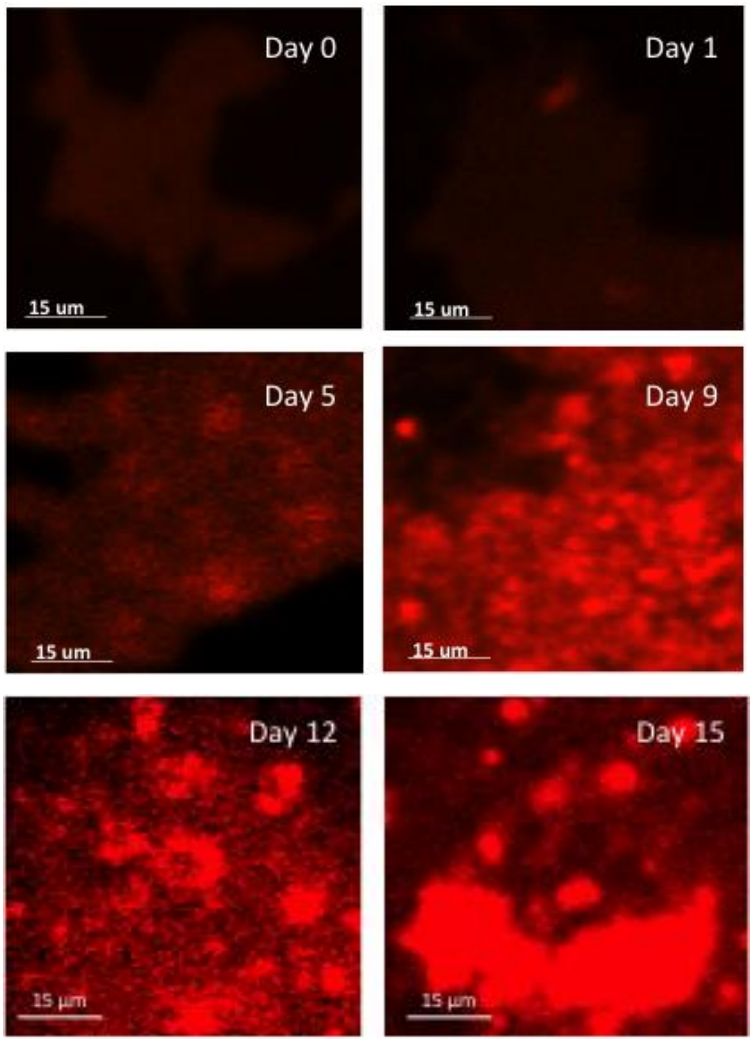


**Figure S11. Impact of thermal annealing on functionalization density of linkers.**
Fluorescence images after GO nanosheets were functionalized with TAMRA fluorophores without including the antibody protein. This experiment was performed to directly probe the linker concentration while discounting the effect of antibodies. The images (day 1 to day 9) reveal increasing florescence with annealing time, indicating denser grafting of the linkers on to the GO substrate. The images (day 9, 12 and 15) show a convergence in the florescence intensity, thus indicating a steady state attainment and a limit in the amount of linker concentration that can be grafted on to the GO substrate has been achieved. As a consequence, we do not expect a significant improvement in the cell capture yield beyond day 9 GO nanosubtrates. Scale bar is 15 $\mu$m for all images.

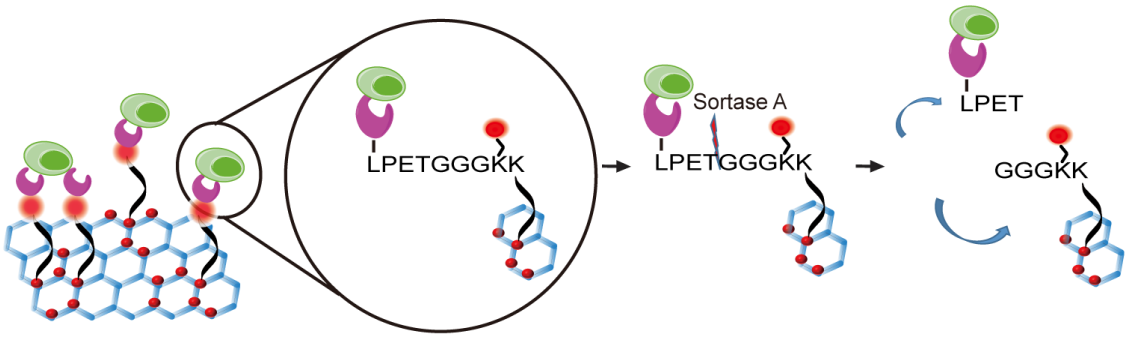


**Figure S12. Schematic of release of captured cells for downstream analyses.**
The release of captured cells can be achieved using a sortase enzyme-cleaved linker (which is attached to the GO substrate) cleaved between the threonine and glycine residues of the peptide to release cells captured from whole blood.

**Table S3: Estimation of the unit cost of the GO-based cell capture device.**

| Raw Material | Purchase Price per unit | Purchase Unit size | Amount required (per device) | Cost (per device) | Remarks (for calculation) |
|---|---|---|---|---|---|
| **GO** | $634.00 | 200 ml | 200 $\mu$l | $0.16 | Diluted, 4× to 1 mg/ml |
| **3-APTES** | $238.00 | 500 ml | 200 $\mu$l | $0.10 | Added as liq., without dilution |
| **EDC** | $311.00 | 25 gm | 1 ml | $0.01 | Added 5× excess, 2 mM in $H_2O$, mol. wt. 115.10 gm |
| **Sulfo-NHS** | $1,376.00 | 5 gm | 1 ml | $0.30 | Added 5× excess, 5 mM in $H_2O$, mol. wt. 217.14 gm |
| **$NH_2$–$(PEG)_{12}$–$NH_2$** | $480.00 | 500 mg | 200 $\mu$l | $0.05 | 0.5 mM in $H_2O$, mol. wt. 544.67 gm |
| **DBCO–NHS ester** | $356.00 | 50 mg | 200 $\mu$l | $0.76 | 1 mM in $H_2O$, mol. wt. 532.50 gm |
| **1% BSA blocking buffer** | $139.00 | 125 ml | 200 $\mu$l | $0.02 | Diluted 10× to 1× TBS |
| **Nanobody** (*E. coli* growth medium) | $40.32 | 1 L | 1 mg | $0.81 | Grown in *E. coli* bioreactors, in LB broth. Yields ~ 40 - 50 mg/L of *E. coli* culture. |
| **Ni-NTA Agarose gel** | $4,353.00 | 500 ml | 1 ml | $1.74 | For purification of nanobody, recycled and used up to 5 times |
| **Microscope glass slide** | $19.30 | 72 units | 2 slides | $0.54 | 2 glass slides mounted together with 2-sided tape, to create cell capture volume of 30 $\mu$l |
| **2-sided tape** | $1.29 | 75” | 2” | $0.03 | For sticking the 2 glass slides |
| **PBS, 1×** | $214.00 | 12 L | 10 ml | $0.18 | For various wash steps |
| | | | **Total Cost** | **$4.69** | Price per unit of cell capture device, Research phase |

Note: The active area of the cell capture device is 12 mm × 25 mm. Therefore, for the coating reactions, a volume of ~ 200 $\mu$l was considered to be sufficient for each component.
All prices quoted in US dollars, and are accurate at the time of publication.

## References

S1. Kim, S.; Zhou, S.; Hu, Y.; Acik, M.; Chabal, Y. J.; Berger, C.; de Heer, W.; Bongiorno, A.; Riedo, E. Room-Temperature Metastability of Multilayer Graphene Oxide Films. *Nat. Mater.* **2012**, *11*, 544–549.

S2. Kumar, P. V.; Bardhan, N. M.; Tongay, S.; Wu, J.; Belcher, A. M.; Grossman, J. C. Scalable Enhancement of Graphene Oxide Properties by Thermally Driven Phase Transformation. *Nat. Chem.* **2014**, *6*, 151–158.

S3. Zhang, M.; Wang, Y.; Huang, L.; Xu, Z.; Li, C.; Shi, G. Multifunctional Pristine Chemically Modified Graphene Films as Strong as Stainless Steel. *Adv. Mater. (Weinheim, Ger.)* **2015**, *27*, 6708–6713.

S4. Liu, Q.; Zhang, M.; Huang, L.; Li, Y.; Chen, J.; Li, C.; Shi, G. High-Quality Graphene Ribbons Prepared from Graphene Oxide Hydrogels and Their Application for Strain Sensors. *ACS Nano* **2015**, *9*, 12320–12326.